ADVANCED FUNCTIONAL MATERIALS

Color Tuning of a Light-Emitting Polymer: Polyfluorene-Containing Pendant Amino-Substituted Distyrylarylene Units**

By *Huei-Jen Su*, *Fang-Iy Wu*, *Ya-Hsien Tseng*, and *Ching-Fong Shu**

We have synthesized a novel polyfluorene copolymer polyfluorene–bis[4-(diphenylamino)styryl]fluorene (PF–DPAS) by orthogonally attaching an amino-substituted distyrylarylene dye bis[4-(diphenylamino)styryl]fluorene, onto the C9 position of a fluorene unit. We have investigated this polymer's thermal properties, electronic properties (viz., absorption and photoluminescence), and electrochemical behavior. Photoluminescence studies indicate that color tuning can be achieved through efficient Förster energy transfer from the higher-energy polyfluorene backbone to the lower-energy pendant DPAS units. We have fabricated light-emitting diodes with the structure indium tin oxide (ITO)/poly(3,4-ethylenedioxythiophene) (PEDOT)/emitting layer/1,3,5-tris(*N*-phenylbenzimidazol-2-yl)benzene (TPBI)/Mg:Ag. The devices, based on blends of PF–DPAS in polyfluorene–triphenylamine–oxadiazole (PF–TPA–OXD), exhibit significant improvements in device performance relative to that of the pure PF–TPA–OXD device; we attributed this improvement to both a red-shift of the electroluminescence (EL) spectra and an enhancement in quantum efficiency. At a blend ratio of 1:20, the EL spectrum is voltage-independent and stable, and exhibits the characteristic emission of a DPAS moiety: a peak at 461 nm and Commission Internationale de l'Eclairage (CIE) coordinates of (0.15, 0.18). The maximum external quantum efficiency is 2.08 % (2.87 cd A^{-1}) at a bias of 9 V (86.1 mA cm^{-2}) with a brightness of 2467 cd m^{-2}; the maximum brightness (6916 cd m^{-2}) occurred at an applied voltage of 13 V and a current density of 361 mA cm^{-2}.

1. Introduction

Organic light-emitting polymers continue to be the subject of intense academic and industrial research because of their potential applications in flat-panel displays.[1] The main advantages of organic polymers, compared to inorganic or molecular organic materials, are the ability to tailor their luminescence properties by manipulating their chemical structure and the feasibility of utilizing spin-coating and printing processes for preparing large-area display devices. Polymers with large energy bandgaps that emit blue light efficiently are of special interest because these materials are desirable either as blue-light sources in full-color displays, or as host materials for generating other colors through energy transfer to lower-energy fluorophores.[2]

Because of their high photoluminescence (PL) and electroluminescence (EL) efficiencies, good thermal stabilities, solubility, and film-forming capabilities, polyfluorenes (PFs) are very promising candidates for preparing blue-light-emitting materials.[3] Facile methods for functionalizing the C9 position of the fluorene unit also offer the possibility of tuning the optoelectronic properties of PFs through macromolecular engineering.[4–6] In conjugated polymers, Förster energy transfer between two chromophore segments that have different energies is fast and efficient, and it shifts the emission to longer wavelengths.[7,8] In addition, such low-energy sites act as effective energy traps for excitons formed at the higher-energy segments.[9] Significant efforts have been made to tune the colors of fluorene-based polymers to longer wavelengths. Most of the color-tunable PF derivatives that have been developed so far have been synthesized by incorporating low-bandgap co-monomers into the PF main chain.[10–12] Only a few studies have been concerned with the attachment of narrow-bandgap dyes as pendant side groups,[12,13] even though this route has the advantage of permitting the incorporation of a high concentration of dyes without affecting the electronic properties of the PF backbone.[12] In this paper, we report the synthesis of a color-tunable fluorene copolymer by orthogonally attaching an amino-substituted distyrylarylene (DSA) dye bis[4-(diphenylamino)-styryl]fluorene (DPAS), onto the C9 position of a fluorene unit. We chose DSA as the side-chain dye because of its intense blue fluorescence and its impressive performance in organic light-emitting diodes (OLEDs).[14] Because of the good spectral overlap between the emission spectrum of PF and the absorption spectrum of the pendant DPAS units, an efficient Förster energy transfer from the higher-energy polymer backbone to the lower-energy side chain occurs, which leads to emission solely, or predominantly, from the latter. Consequently, the PL of the copolymer is fine-tuned to the blue region and the maximum wavelength, λ_{max}, of the emission is red-shifted from 418 nm for poly(dialkylfluorene)[15] (which is located at a wavelength where the human eye is not very sensitive) to 467 nm (which is closer to the maximum of a relative photopic luminous efficiency function).[16] This moderate red-shift, in turn, results in a higher luminance efficiency. The fluorene co-

[*] Prof. C.-F. Shu, H.-J. Su, F.-I. Wu, Y.-H. Tseng
Department of Applied Chemistry, National Chiao Tung University
Hsinchu 300, Taiwan (R. O. China)
E-mail: shu@cc.nctu.edu.tw

[**] We thank the National Science Council for financial support. Our special thanks go to Professor C.-H. Cheng, Dr. J.-P. Duan, and Dr. H.-T. Shih for their support and cooperation during the preparation and characterization of the light-emitting devices.

 DOI: 10.1002/adfm.200400269

polymer, when used as a dopant in polymer light-emitting diodes, gives a bright blue emission from the dopant.

2. Results and Discussion

2.1. Polymer Synthesis and Characterization

Scheme 1 illustrates the synthetic route we followed for preparing the DPAS monomer containing a spirobifluorene skeleton. Starting from 2,7-dibromo-9-fluorenone, the precursor 2,7-dibromo-9,9′-spirobifluorene (**1**) was synthesized and then bromomethylated to give 2,7-dibromo-2′,7′-bis(bromomethyl)-9,9′-spirobifluorene (**2**), according to reported procedures.[17,18] Subsequent Arbuzov reaction with triethyl phosphite yielded the phosphonate ester (**3**).[18] The Horner–Emmons reaction of **3** with 4-diphenylaminobenzaldehyde, conducted in tetrahydrofuran (THF) using potassium *tert*-butoxide as the base, afforded the desired monomer, 2,7-dibromo-2′,7′-bis[4-(diphenylamino)styryl]-9,9′-spirobifluorene (**4**). The structure of monomer **4** was confirmed by ^{1}H and ^{13}C NMR spectroscopy. The vinylic protons gave rise to an AB quartet at δ 6.84/6.87 with a coupling constant of 16.0 Hz, which indicates a trans configuration. The signal for a quarternary carbon atom at δ 65.4 (C9) revealed the presence of the spiro skeleton. High-resolution mass spectrometric and elemental analysis data provided additional verification of the proposed structure.

We synthesized the polyfluorene copolymer PF–DPAS by performing a Suzuki coupling reaction between the dibromides **4** and **5** and the diboronate **6** in a mole ratio of 1:1:2 (Scheme 2).[19,20] This copolymerization was undertaken using $Pd(PPh_3)_4$ as the catalyst in a mixture of toluene, and 2.0 M aqueous K_2CO_3 in the presence of aliquate 336 as a phase-transfer reagent.[11a,d] When polymerization was complete, the end groups of the polymer chain were capped by heating under reflux sequentially with phenylboronic acid and bromobenzene. The structure of PF–DPAS was characterized by ^{1}H and ^{13}C NMR spectroscopy. The ratio of integrals between the aliphatic and aromatic protons was quite consistent with the monomer feed ratio. In the ^{13}C NMR spectrum, two signals at δ 55.3 and 66.1 corresponded to the C9 carbon atoms of the two different fluorene units in PF–DPAS.

The polyfluorene copolymer PF–DPAS was readily soluble in common organic solvents, such as toluene, chlorobenzene, chloroform, and THF. The molecular weights of the polymer were determined by gel permeation chromatography (GPC) using THF as the eluent and calibrating against polystyrene standards. This polymer possessed a weight-average molecular weight (M_w) of ca. 3.3×10^4 g mol^{-1} with a polydispersity index of 2.9. The thermal properties of PF–DPAS were investigated by differential scanning calorimetry (DSC) and thermogravimetric analysis (TGA). We observed a distinct glass-transition temperature (T_g) at 145 °C, which is much higher than that of poly(9,9-dioctylfluorene) (POF; T_g = ca. 75 °C).[21] It is evident that incorporating rigid diphenylaminostyryl–spirobifluorene units into the polymer backbone enhances the rigidity of the chain and increases T_g. A relatively high value of T_g, which can prevent morphological change and suppress the formation of aggregates and excimers upon exposure to heat, is an essential characteristic of polymers if they are to be used as emissive materials in light-emitting applications.[22] As revealed by TGA, PF–DPAS also exhibits good thermal stability; its 5 % weight loss occurred at 420 °C.

2.2. Photophysical Properties

We measured the optical properties of the DPAS-containing fluorene copolymer, both in dilute solution and in the solid state. Figure 1 presents these spectra and Table 1 summarizes the spectral data. The absorption and PL spectra of compound **4**, which serves as a model compound for studying the

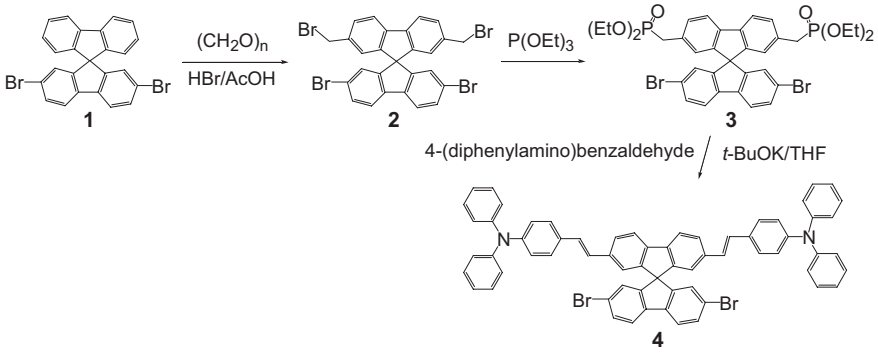

Scheme 1. Synthesis of DPAS.

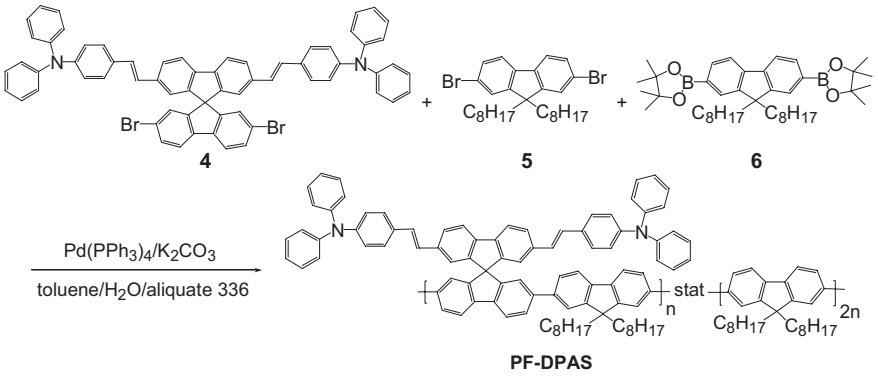

Scheme 2. Synthesis of PF–DPAS.

ADVANCED FUNCTIONAL MATERIALS

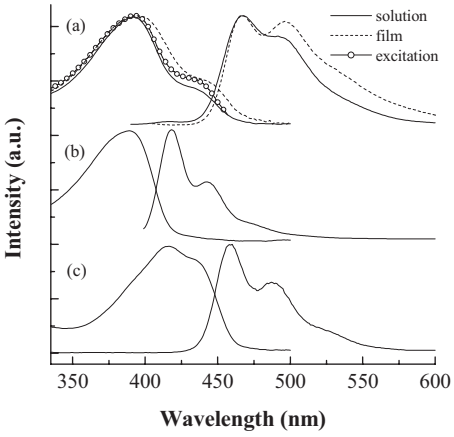

Figure 1. a) UV-vis absorption and PL spectra of PF–DPAS in $CHCl_3$ solution and in the solid state, and excitation spectra of PF–DPAS in $CHCl_3$ solution. UV-vis absorption and PL spectra of b) POF and c) **4** in $CHCl_3$.

optical properties of the DPAS moieties, are also displayed in Figure 1. In chloroform solution, PF–DPAS exhibits a main absorption peak at 393 nm with an absorption shoulder peak appearing at the longer wavelength, 434 nm. By comparing this spectrum with the absorption spectra of POF and compound **4**, we ascribe the 393 nm band to a π–π* transition derived from the conjugated polyfluorene backbone, and assign the shoulder at longer wavelength to the absorption originating from the pendant DPAS groups. Upon excitation of the PF main chain at 380 nm, the emission spectrum displays an emission band at 467 nm combined with a shoulder at 489 nm. There is almost no luminescence from the PF backbone that can be detected in the deep-blue region (400–440 nm). The PL spectrum, which is nearly identical to that of compound **4** (λ_{max} = 459, 487 nm), can be attributed to emission from the pendant DPAS units. This result suggests that efficient Förster energy transfer occurs as a consequence of good spectral overlap between the emission spectrum of the polymer backbone and the absorption spectrum of the diphenylaminostyryl derivative (Figs. 1b,c).[7] Consequently, most excitons formed in the PF main chain by direct photoexcitation are likely to migrate to the lower-energy pendant groups, from which emission occurs. The fact that we observed near-complete quenching of the PF emission even in a very dilute solution (10^{-6} M) indicates that efficient intrachain energy transfer takes place in the PF–DPAS copolymer, as a result of its large DPAS content (25 mol-%). In addition, the excitation spectrum of PF–DPAS, monitored at 467 nm, is a perfectly superimposed image of the absorption spectrum. Again, this observation reveals that energy transfer from the excited PF backbone to the pendant groups is very efficient and contributes significantly to the emission intensity of the DPAS side chain. We measured the PL quantum yield (Φ_f) of PF–DPAS in toluene, excited at 365 nm, to be 0.75 relative to a 9,10-diphenylanthrancene (Φ_f = 0.9) standard,[23] which is close to the fluorescence yield measured for POF (Φ_f = 0.85).

When compared with its corresponding spectra in dilute solution, the absorption and PL spectra of the PF–DPAS thin film are broadened and slightly red-shifted, and the intensity of the emission peak at 497 nm, which reflects the 0–1 transition, increases. The spectral changes observed in this thin film are probably the result of aggregate formation and π–π interactions of the chromophores in the solid state. We note that the emission from the PF backbone is completely suppressed in the PF–DPAS film; instead, the PL spectrum reveals only the emission from the pendent DPAS units. The lack of polyfluorene emission in the film indicates that complete energy transfer is facilitated by both the intra- and interchain interactions resulting from the shorter distances between polymer chains in the solid state. By comparison with the fluorescence intensity of the POF polymer thin-film sample (Φ_f = 0.55),[24] we estimated the PL quantum yield of the PF–DPAS film excited at 380 nm to be 0.19. The lower quantum efficiency might be the result of excimer formation induced by π–π interactions of the chromophores in the solid state, because of the large content of DPAS moieties in the copolymer (vide infra).

The fluorene copolymer PF–DPAS was designed to be a blue-light-emitting material with a high emissive efficiency, but this polymer turned out to exhibit blue emission only in solution. In the pure solid-film state, the emission shifted to the blue-green region and also exhibited a lower quantum efficiency, which was probably due to the formation of intermolecular species, i.e., aggregates and excimers. To investigate excimer formation in the solid state, we blended PF–DPAS with polyfluorene–triphenylamine–oxadiazole (PF–TPA–OXD) in toluene to yield a homogeneous solution, from which we then cast a solid film. PF–TPA–OXD, which is a highly efficient blue-light-emitting fluorene copolymer, possesses bulky hole-transporting triphenylamine (TPA) and electron-transporting oxadiazole (OXD) pendant groups at the C9 positions of the fluorene units.[6b] These bipolar substituents can act to both suppress aggregation and improve charge injection.[6b,25] As indicated in Figure 2, the absorption spectrum of a PF–DPAS/PF–TPA–OXD blend film (1:5, w/w) exhibits two characteristic bands at 390 and 306 nm, which we attribute to the absorptions of the PF backbones in the blended material and the absorptions of the pendent TPA and OXD units in the host poly-

Table 1. Optical properties and quantum yields of PF–DPAS, **4**, and POF. Peaks that appear as shoulders or weak bands are listed in parentheses. Φ_f: PL quantum yield.

	Solution [a]			Film [b]		
	Abs [nm]	PL [c] [nm]	Φ_f [d]	Abs [nm]	PL [c] [nm]	Φ_f
PF–DPAS	393 (434)	467 (489)	0.75	393 (438)	467, 497	0.19 [e]
4	416 (435)	459 (487)				
POF	389	418 (442)	0.85	387	424 (448)	0.55

[a] Evaluated in chloroform. [b] Prepared by spin-coating from a toluene solution. [c] Excited at 380 nm. [d] Determined in toluene relative to 9,10-diphenylanthracene in cyclohexane (Φ_f = 0.9), with excitation at 365 nm. [e] Relative to the thin-film quantum efficiency of POF (Φ_f = 0.55), with excitation at 380 nm.

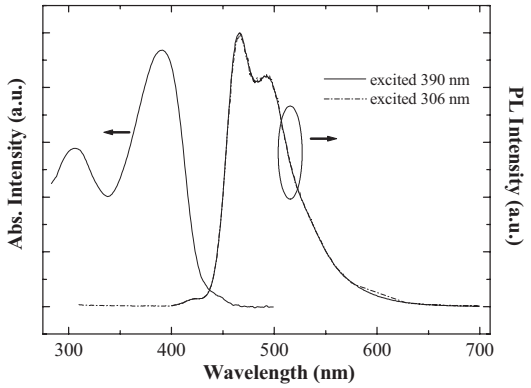

Figure 2. UV-vis absorption and PL spectra of a blend of PF–DPAS and PF–TPA–OXD (1:5, w/w).

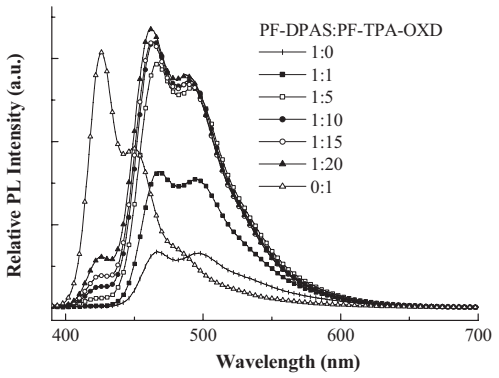

Figure 3. PL spectra of PF–DPAS and PF–TPA–OXD films, and of blend films with weight ratios of 1:1, 1:5, 1:10, 1:15, and 1:20 that correspond to molar ratios of DPAS to fluorene units of 13.5:100, 4.7:100, 2.6:100, 1.8:100, and 1.4:100, respectively.

mer, respectively; the absorption of the DPAS moieties at 435 nm becomes obscure because of the dilution effect. Upon excitation at 390 nm, the PL spectrum resembles that of PF–DPAS in dilute solution, which we ascribe to the singlet excited states of the single chain. The formation of interchain species is completely suppressed as a result of the dilution effect induced by the host polymer. In addition, the reduced concentration of DPAS moieties in the blend also imparts a significant increase, i.e., a 3.7-fold enhancement, in the PL quantum efficiency of the material. Obviously, the concentration quench of DPAS in the pure PF–DPAS film limits its PL efficiency, and the solid-state dilution in the PF–TPA–OXD host could separate the DPAS moieties, thus enhancing the PL efficiency. We note that only a trace amount of the emission originates from the PF backbone, even though the content of DPAS in this blend decreased to a molar ratio of DPAS to fluorene units of 4.7:100 (cf. a ratio of 25:100 for the pure PF–DPAS polymer). This outcome reveals, once again, that Förster energy transfer from the excited PF backbone to the DPAS groups is very efficient. Moreover, upon irradiation at 306 nm, a wavelength we attribute to the absorptions of the pendent TPA and OXD units in the host polymer, the blended film also exhibits a blue emission with a PL spectrum that is perfectly superimposable with that obtained under excitation of the PF backbone at 390 nm. There is no luminescence from the TPA and OXD side chains detectable at ca. 360 nm.[6b] These observations indicate that, besides the direct energy transfer from the excited PF main chain to the pendant DPAS units, an efficient cascade energy transfer takes place in the blended material from the excited TPA and OXD substituents of the host polymer, to the pendant DPAS units of the doping polymer, which is mediated by the PF backbone. Figure 3 presents PL spectra of PF–TPA–OXD films blended with various amounts of PF–DPAS. The intensity of emission has been corrected with the absorbance at the excitation wavelength (390 nm). It is noteworthy that, upon reducing the doping concentration, the emission intensity rises and reaches a plateau at a concentration of ca. 5 wt.-%, and a shoulder at 426 nm appears, which we attribute to emission from the PF backbone as a result of incomplete energy transfer.

2.3. Electrochemistry

We investigated the electrochemical behavior of PF–DPAS in solution by cyclic voltammetry, using ferrocene as the internal standard. The results are displayed in Figure 4. During the anodic scan in CH_2Cl_2, we observe a reversible oxidation at 0.35 V ($E^{o\prime}$), with the onset potential at 0.27 V, followed by an irreversible oxidation with a peak potential at 0.81 V. In the cathodic sweep in THF, we detect an irreversible reduction process with an onset potential at –2.46 V. Comparison with the cyclic voltammograms of compound **4** and POF (Figs. 4b,c) reveals that the first reversible oxidation originates from the DPAS side chain and the second irreversible oxidation derives from the PF backbone, whereas the reductive process is a combination of the reductions of both the backbone and pendant groups, and arises from overlap of their reduction potentials.

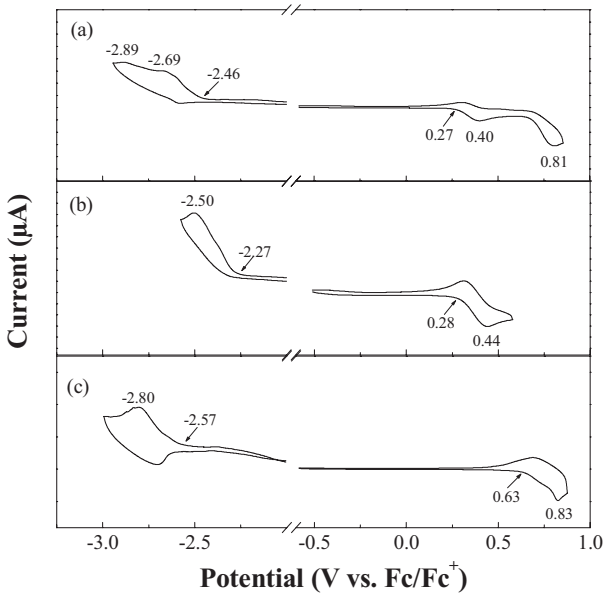

Figure 4. Cyclic voltammograms of a) PF–DPAS, b) compound **4**, and c) POF.

ADVANCED FUNCTIONAL MATERIALS

The electrochemical measurements reveal that both the DPAS side chains and the PF main chain do retain their own electronic characteristics in the copolymer.

2.4. EL Properties of LEDs

To facilitate device performance and efficiency, we fabricated a triple-layered diode with a 1,3,5-tris(*N*-phenylbenzimidazol-2-yl)benzene (TPBI) electron injection/transport layer (ETL), introduced between the light-emitting layer and the Mg:Ag cathode, for hole blocking and exciton confinement.[26] Figure 5 displays the EL spectra of a device that has the configuration indium tin oxide (ITO)/poly(3,4-ethylenedioxythiophene) (PEDOT)/polymer/TPBI/Mg:Ag; these spectra are quite similar to the PL spectra discussed previously (Fig. 3) for

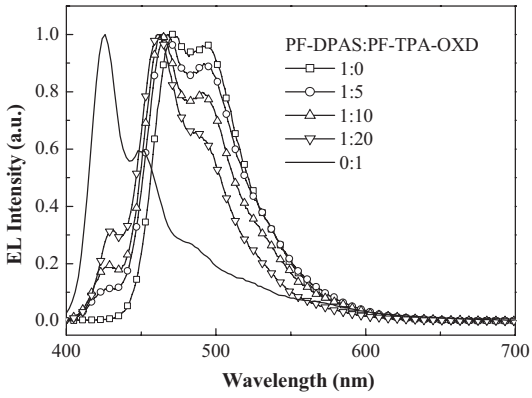

Figure 5. EL spectra of ITO/PEDOT/polymer/TPBI/Mg:Ag devices.

PF–DPAS, PF–TPA–OXD, and their blends. Compared with the broad emission from the device prepared from pristine PF–DPAS, the phenomena of blue-shifting and band narrowing of the EL spectra obtained for the blends are more pronounced as the amount of PF–TPA–OXD increases. For the 1:20 blend, the full width at half maximum (FWHM) of the EL spectrum is 56 nm, which is 8 nm less than that that of pure PF–DPAS, and the main peak at 461 nm undergoes a blue-shift of as much as 10 nm from that of the device prepared from PF–DPAS only. All of the blends exhibit a shoulder at 425 nm, which is due to incomplete energy transfer from PF–TPA–OXD.

The current-density–voltage characteristics and luminance–voltage characteristics of the LEDs are presented in Figures 6a,b, respectively. As displayed in Figure 6a, the operating voltage of the blend device is higher than that of the device made from PF–DPAS only, but it is close to that of the device made from only PF–TPA–OXD. Both PF–DPAS and PF–TPA–OXD have the same PF backbones, but have DPAS and TPA, respectively, as the hole-transporting side chains. On the other hand, the pendant OXD groups of PF–TPA–OXD possess hole-blocking ability, which may result in an increase of the operating voltage for PF–TPA–OXD-containing devices.[27] The turn-on voltage of the

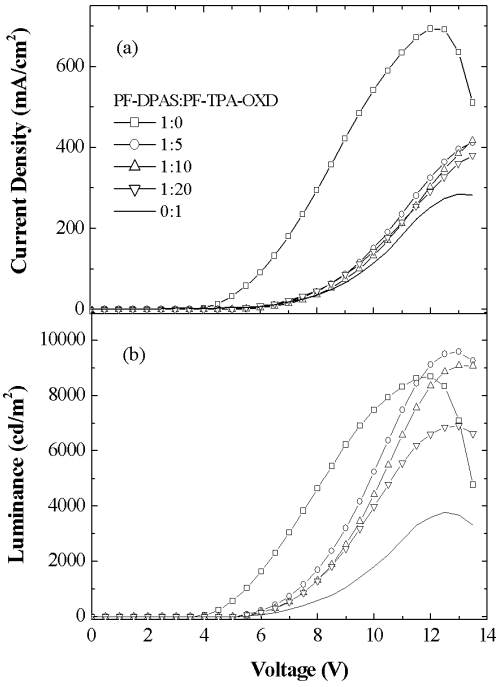

Figure 6. Plots of a) current density versus applied voltage and b) luminance versus applied voltage of ITO/PEDOT/polymer/TPBI/Mg:Ag devices.

PF–DPAS-only device is 3.4 V (corresponding to 1 cd m^{-2}) with a maximum brightness of 8697 cd m^{-2} at 12 V; the emission, however, lies in the blue–green region. Table 2 summarizes the performance of these devices. Although the maximum brightness of the 1:20 device is only 6916 cd m^{-2}, which is less than that for the 1:5 device (9585 cd m^{-2}) or the 1:10 device (9090 cd m^{-2}), the color of the 1:20 device is closer to pure blue, in accordance with the Commission Internationale de l'Eclairage (CIE) color coordinates. Figure 7 demonstrates that the 1:20 device exhibits a voltage-independent and stable EL spectrum. In contrast, polydialkylfluorene-based EL devices show an intense additional band between 500 and 600 nm during device operation, leading to the instability in emission color.[28] Figure 8 indicates that the external quantum efficiencies of the blends are similar to each other and are higher than that of the device prepared from PF–DPAS alone. This result is consistent with the observations (Fig. 3) we made for the PL process. In addition, the devices based on blends of PF–DPAS in PF–TPA–OXD are noteworthy, in that they exhibit significant improvements in device performance when compared with the host-only PF–TPA–OXD device. The higher luminance efficiency of the blend-based device might be due to a red-shift of the EL spectrum, relative to that obtained from the device based on PF–TPA–OXD, so that it becomes closer to the maximum of the relative photopic luminous efficiency function.[16] For the blend ratio of 1:20, the peak of the EL spectrum is shifted to 461 nm, which corresponds to color coordinates of (0.15, 0.18), which are still located in the blue region of the electromagnetic spectrum where the human eye is more sensitive, compared to the purple–blue color emitted by the PF–TPA–OXD-based device (λ_{max} = 426 nm). This shift is accompanied by

Table 2. Performances of devices with the structure ITO/PEDOT/EML/TPBI/Mg:Ag (EML: emitting layer). The data in parentheses were recorded at 100 mA cm^{-2}.

PF–DPAS/PF–TPA–OXD [by weight]	1:0	1:5	1:10	1:20	0:1
Turn-on voltage [V] [a]	3.4	5.0	5.0	5.0	4.7
Voltage [V] [b]	4.7 (6.1)	7.0 (9.2)	6.2 (9.5)	6.9 (9.3)	7.1 (9.7)
Brightness [cd m^{-2}] [b]	350 (1775)	774 (3611)	708 (3423)	487 (2843)	295 (1590)
Luminance efficiency [cd A^{-1}] [b]	1.75 (1.78)	3.87 (3.62)	3.54 (3.42)	2.42 (2.85)	1.46 (1.59)
External quantum efficiency [%] [b]	0.88 (0.89)	2.07 (1.94)	2.10 (2.03)	1.75 (2.06)	1.07 (1.16)
Maximum brightness [cd m^{-2}]	8697 @ 12 V	9585 @ 13 V	9090 @ 13 V	6916 @ 13 V	3769 @ 12.5 V
Maximum luminance efficiency [cd A^{-1}] (cd/A)	1.79	3.88	3.60	2.87	1.66
Maximum external quantum efficiency [%]	0.90	2.08	2.13	2.08	1.21
EL maximum [nm] [c]	471	468	463	461	426
CIE coordinates, *x* and *y* [c]	0.14 and 0.32	0.15 and 0.27	0.15 and 0.24	0.15 and 0.18	0.18 and 0.12

[a] At 1 cd m^{-2}. [b] At 20 mA cm^{-2}. [c] At 11 V.

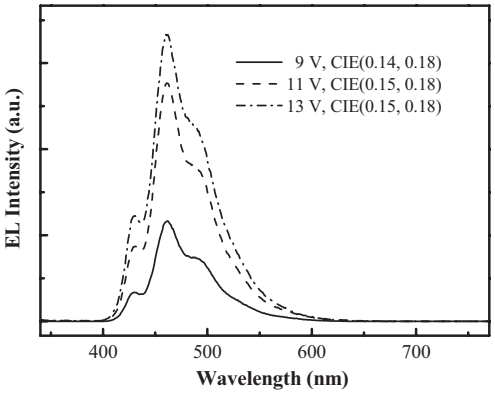

Figure 7. EL spectra of a device based on a blend of PF–DPAS and PF–TPA–OXD (1:20, w/w) at various voltages.

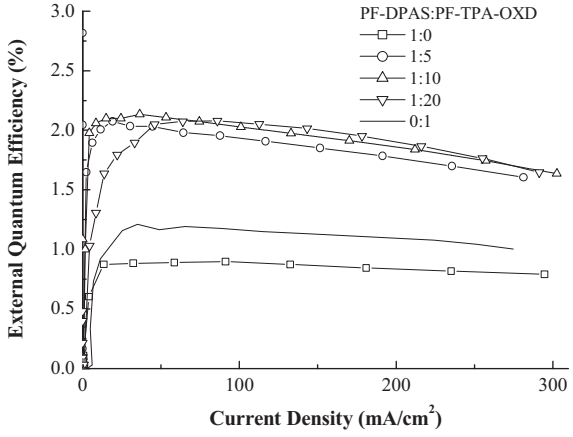

Figure 8. External quantum efficiency versus current density of the ITO/PEDOT/polymer/TPBI/Mg:Ag device.

an improvement in the external quantum efficiency (to 2.08 %) induced by the dilution effect.

3. Conclusion

We have synthesized a polyfluorene copolymer (PF–DPAS) containing pendant amino-substituted DSA dye units that are orthogonally attached to the C9 positions of fluorene units. The presence of the rigid, spiro, pendant units increase imparts a substantial increase to the glass-transition temperature of the material. PL studies demonstrate that most of the excitons formed in the PF main chain by direct photoexcitation migrate to the lower-energy pendant groups, from which emission occurs. In addition, in the PF–DPAS/PF–TPA–OXD blend, an efficient cascade energy transfer takes place from the excited TPA and OXD substituents of the host polymer to the pendent DPAS units of the doping polymer, mediated by the PF backbone. Because of color tuning as well as enhancements in quantum efficiency, the EL devices based on blends of PF–DPAS in PF–TPA–OXD exhibit significant improvements in device performance compared to the pure PF–TPA–OXD device. The device prepared at a blend ratio of 1:20 displays the characteristic emission spectrum of the amino-substituted DSA dye and exhibits a voltage-independent and stable EL spectrum with a peak at 461 nm, which corresponds to CIE color coordinates of (0.15, 0.18), located in the pure-blue region. The maximum external quantum efficiency of 2.08 % (2.87 cd A^{-1}), with a brightness of 2467 cd m^{-2}, was obtained at a current density of 86.1 mA cm^{-2}, and the maximum brightness of 6916 cd m^{-2} was achieved at an applied voltage of 13 V.

4. Experimental

Materials: 2,7-Dibromo-9,9′-spirobifluorene (**1**) [17], 2,7-dibromo-2′,7′-bis(bromomethyl)-9,9′-spirobifluorene (**2**) [18], 2,7-dibromo-2′,7′-bis(diethylphosphorylmethyl)-9,9′-spirobifluorene (**3**) [18], 2,7-dibromo-9,9-dioctylfluorene (**5**) [20], 2,7-bis(4,4,5,5-tetramethyl-1,3,2-dioxaborolane-2-yl)-9,9-dioctylfluorene (**6**) [20], and the electron-transport material 1,3,5-tris(*N*-phenylbenzimidazol-2-yl)benzene (TPBI) [29] were synthesized as reported previously. The solvents were dried using

standard procedures. All other reagents were used as received from commercial sources, unless otherwise stated.

*2,7-Dibromo-2′,7′-bis[4-(diphenylamino)styryl]-9,9′-spirobifluorene (**4**)*: Potassium *tert*-butoxide (147 mg, 1.16 mmol) was added to a solution of **3** (300 mg, 390 μmol) and 4-diphenylaminobenzaldehyde (265 mg, 970 μmol) in anhydrous THF (3 mL) under a nitrogen atmosphere. The mixture was heated under reflux for 2 h, cooled, and then added to water (100 mL). The precipitate was washed with hexane and purified by recrystallization from $CHCl_3$ to afford **4** (315 mg, 79.7 %). ^{1}H NMR (500 MHz, $CDCl_3$): δ 6.78 (s, 2 H), 6.84 (AB, J = 16.0 Hz, 2 H), 6.87 (AB, J = 16.0 Hz, 2 H), 6.89 (d, J = 1.5 Hz, 2 H), 6.95–7.01 (m, 10 H), 7.06 (d, J = 8.0 Hz, 8 H), 7.21 (d, J = 8.0 Hz, 6 H), 7.25 (d, J = 8.5 Hz, 4 H), 7.51 (d, J = 8.0 Hz, 4 H), 7.70 (d, J = 8.5 Hz, 2 H), 7.77 (d, J = 8.0 Hz, 2 H). ^{13}C NMR (75 MHz, $CDCl_3$): δ 65.4, 120.4, 121.4, 121.5, 122.0, 123.0, 123.3, 124.5, 126.5, 126.9, 127.2, 127.5, 128.2, 129.2, 131.2, 131.2, 137.6, 139.6, 140.6, 147.3, 147.4, 147.9, 150.5. High-resolution mass spectrometry (HRMS) $[M^+ + H]$ calcd. for $C_{65}H_{45}N_2{}^{79}Br_2$, 1011.1949; found 1011.1951. Anal. Calcd. for $C_{65}H_{44}N_2Br_2$: C, 77.08; H, 4.38; N, 2.77. Found: C, 76.92; H, 4.42; N, 2.70.

Preparation of PF–DPAS: Aqueous potassium carbonate (2.0 M, 2.5 mL) and aliquate 336 (ca. 12 mg) were added to a solution of the monomers **4** (150 mg, 148 μmol), **5** (81.2 mg, 148 μmol), and **6** (191 mg, 296 μmol) in toluene (4.0 mL). This solution was degassed and tetrakis(triphenylphosphine)palladium (9 mg, 2.6 mol-%) was added in one portion under a nitrogen atmosphere. The solution was heated under reflux at 110 °C under nitrogen for 8 h. The end groups were capped by refluxing for 12 h each with phenylboronic acid (75.8 mg, 620 μmol) and bromobenzene (97.7 mg, 620 μmol). After this period, the mixture was cooled and poured into a mixture of methanol and water (150 mL, 1:1 v/v). The crude polymer was filtered, washed with excess methanol, and dried. The polymer was dissolved in $CHCl_3$ (4.0 mL), filtered, and precipitated into methanol (150 mL). The precipitate was collected, washed with acetone for 24 h using a Soxhlet apparatus, and dried under vacuum to give PF–DPAS (283 mg, 94.8 %). ^{1}H NMR (300 MHz, $CDCl_3$): δ 0.75–0.78 (m, 30 H), 1.04–1.11 (m, 60 H), 2.07 (br, 12 H), 6.89–7.09 (m, 26 H), 7.18–7.20 (m, 10 H), 7.33–7.65 (m, 20 H), 7.80–7.83 (m, 4 H), 7.98 (s, 2 H). ^{13}C NMR (75 MHz, $CDCl_3$): δ 14.1, 22.49, 22.54, 22.58, 23.9, 29.0, 29.1, 29.2, 29.9, 30.0, 31.6, 31.7, 31.8, 40.3, 55.3, 66.1, 119.8, 119.9, 120.2, 121.5, 121.9, 122.7, 123.0, 123.3, 124.5, 126.1, 126.8, 127.2, 128.0, 128.7, 128.8, 129.2, 131.3, 137.4, 139.7, 140.0, 140.4, 140.9, 141.5, 147.2, 147.4, 149.6, 149.8, 151.6, 151.8. Anal. Calcd. for $C_{152}H_{164}N_2$: C, 90.42; H, 8.19; N, 1.39. Found: C, 89.00; H, 7.87; N, 1.16.

Characterization: ^{1}H and ^{13}C NMR spectra were recorded on either a Varian Unity Yinova 500 MHz or a Bruker-DRX 300 MHz spectrometer. Mass spectra were obtained on a JEOL JMS-SX/SX 110 mass spectrometer. Gel permeation chromatography (GPC) was performed on a Waters chromatography unit interfaced with a Waters 410 differential refractometer, using three 5 μm Waters styragel columns (300 × 7.8 mm) connected in series in order of decreasing pore size (10^4, 10^3, and 10^2 Å); THF was the eluent, and standard polystyrene samples were used for calibration. Differential scanning calorimetry (DSC) was performed on a SEIKO EXSTAR 6000DSC unit at a heating rate of 20 °C min^{-1} and a cooling rate of 40 °C min^{-1}. Samples were scanned from 30 to 300 °C, cooled to 0 °C, and then scanned again from 30 to 300 °C. The glass transition temperatures (T_g) were determined from the second heating scan. Thermogravimetric analysis (TGA) was undertaken on a DuPont TGA 2950 instrument. The thermal stability of each sample under a nitrogen atmosphere was determined by measuring its weight loss while heating at a rate of 20 °C min^{-1}. Ultraviolet-visible (UV-vis) spectra were measured using an HP 8453 diode-array spectrophotometer. Photoluminescence (PL) spectra were obtained on a Hitachi F-4500 luminescence spectrometer. Cyclic voltammetry (CV) measurements were performed using a BAS 100 B/W electrochemical analyzer. The oxidation and reduction measurements were undertaken, respectively, in anhydrous CH_2Cl_2 and anhydrous THF, containing 0.1 M $TBAPF_6$ as the supporting electrolyte, at a scan rate of 50 mV s^{-1}. The potentials were measured against an Ag/Ag^+ (0.01 M $AgNO_3$) reference electrode, using ferrocene as the internal standard.

Fabrication of Light-Emitting Devices: We fabricated LED devices having the structure ITO/poly(styrene sulfonate)-doped poly(3,4-ethylenedioxythiophene) (PEDOT) (35 nm)/doped emitting layer (50–70 nm)/TPBI (30 nm)/Mg:Ag (100 nm)/Ag(100 nm). The PEDOT was spin-coated directly onto the ITO glass and dried at 80 °C for 12 h under vacuum to improve hole injection and substrate smoothness. The light-emitting layer was spin-coated on top of the PEDOT layer, using toluene as the solvent, and then dried for 3 h at 60 °C under vacuum. Prior to film casting, the polymer solution was filtered through a Teflon filter (0.45 μm). The TPBI layer was grown by thermal sublimation under vacuum (3×10^{-6} torr) and was used as an electron transporting layer, which would also block holes and confine excitons [21]. Subsequently, the cathode Mg:Ag (10:1, 100 nm) alloy was deposited by coevaporation onto the TPBI layer and then an additional Ag protection layer (100 nm) was placed onto the alloy. Current–voltage–luminance was measured under ambient conditions using a Keithley 2400 source meter and a Newport 1835C optical meter equipped with an 818ST silicon photodiode.

Received: June 21, 2004
Final version: February 17, 2005

[1] a) A. Kraft, A. C. Grimsdale, A. B. Holmes, *Angew. Chem. Int. Ed.* **1998**, *37*, 402. b) R. H. Friend, R. W. Gymer, A. B. Holmes, J. H. Burroughes, R. N. Marks, C. Taliani, D. D. C. Bradley, D. A. Dos Santos, J. L. Brédas, M. Lögdlund, W. R. Salaneck, *Nature* **1999**, *397*, 121. c) M. T. Bernius, M. Inbasekaran, J. O'Brien, W. Wu, *Adv. Mater.* **2000**, *12*, 1737. d) U. Mitschke, P. Bäurele, *J. Mater. Chem.* **2000**, *10*, 1471.

[2] a) J. Kido, K. Hongawa, K. Okuyama, K. Nagai, *Appl. Phys. Lett.* **1994**, *64*, 815. b) M. D. McGehee, T. Bergstedt, C. Zhang, A. P. Saab, M. B. O'Regan, G. C. Bazan, V. I. Srdanov, A. J. Heeger, *Adv. Mater.* **1999**, *11*, 1349. c) J. Liu, Y. Shi, Y. Yang, *Appl. Phys. Lett.* **2001**, *79*, 578. d) F.-C. Chen, Y. Yang, M. E. Thompson, J. Kido, *Appl. Phys. Lett.* **2002**, *80*, 2308.

[3] a) Q. Pei, Y. Yang, *J. Am. Chem. Soc.* **1996**, *118*, 7416. b) M. Leclerc, *J. Polym. Sci., Part A: Polym. Chem.* **2001**, *39*, 2867. c) D. Neher, *Macromol. Rapid Commun.* **2001**, *22*, 1365. d) S. Becker, C. Ego, A. C. Grimsdale, E. J. W. List, D. Marsitzky, A. Pogantsch, S. Setayesh, G. Leising, K. Müllen, *Synth. Met.* **2002**, *125*, 73.

[4] a) S. Setayesh, A. C. Grimsdale, T. Weil, V. Enkelmann, K. Müllen, F. Meghdadi, E. J. W. List, G. Leising, *J. Am. Chem. Soc.* **2001**, *123*, 946. b) D. Marsitzky, R. Vestberg, P. Blainey, B. T. Tang, C. J. Hawker, K. R. Carter, *J. Am. Chem. Soc.* **2001**, *123*, 6965. c) H.-Z. Tang, M. Fujiki, Z.-B. Zhang, K. Torimitsu, M. Motonaga, *Chem. Commun.* **2001**, 2426. d) C.-H. Chou, C.-F. Shu, *Macromolecules* **2002**, *35*, 9673. e) J.-H. Lee, D.-H. Hwang, *Chem. Commun.* **2003**, 2836. f) F.-I. Wu, R. Dodda, Jakka, K. J.-H. Huang, C.-S. Hsu, C.-F. Shu, *Polymer* **2004**, *45*, 4257.

[5] a) C. Ego, A. C. Grimsdale, F. Uckert, G. Yu, G. Srdanov, K. Müllen, *Adv. Mater.* **2002**, *14*, 809. b) A. Pogantsch, F. P. Wenzl, E. J. W. List, G. Leising, A. C. Grimsdale, K. Müllen, *Adv. Mater.* **2002**, *14*, 1061.

[6] a) F.-I. Wu, D. S. Reddy, C.-F. Shu, M. S. Liu, A. K.-Y. Jen, *Chem. Mater.* **2003**, *15*, 269. b) C.-F. Shu, R. Dodda, F.-I. Wu, M. S. Liu, A. K.-Y. Jen, *Macromolecules* **2003**, *36*, 6698.

[7] T. Förster, *Discuss. Faraday Soc.* **1959**, *27*, 7.

[8] a) J. Kido, H. Shionoya, K. Nagai, *Appl. Phys. Lett.* **1995**, *67*, 2281. b) S. Tasch, E. J. W. List, C. Hochfilzer, G. Leising, *Phys. Rev. B: Condens. Matter Mater. Phys.* **1997**, *56*, 4479. c) T. Virgilli, D. G. Lidzey, D. D. C. Bradley, *Adv. Mater.* **2000**, *12*, 58.

[9] G. He, J. Liu, Y. Li, Y. Yang, *Appl. Phys. Lett.* **2002**, *80*, 1891.

[10] a) J.-I. Lee, G. Klaerner, M. H. Davey, R. D. Miller, *Synth. Met.* **1999**, *102*, 1087. b) B. Tsuie, J. L. Reddinger, G. A. Sotzing, J. Soloducho, A. R. Katritzky, J. R. Reynolds, *J. Mater. Chem.* **1999**, *9*, 2189. c) A. Donat-Bouillud, I. Lévesque, Y. Tao, M. D'Iorio, *Chem. Mater.* **2000**, *12*, 1931. d) B. Liu, W. L. Yu, Y. H. Lai, W. Huang, *Macromolecules* **2000**, *33*, 8945. e) A. Charas, N. Barbagallo, J. Morgado, L. Alcacer,

Synth. Met. **2001**, *122*, 23. f) I. Lévesque, A. Donat-Bouillud, Y. Tao, M. D'Iorio, S. Beaupré, P. Blondin, M. Ranger, J. Bouchard, M. Leclerc, *Synth. Met*. **2001**, *122*, 79. g) M. Leclerc, *J. Polym. Sci*., *Part A*: *Polym. Chem*. **2001**, *39*, 2867. h) B. Liu, W. L. Yu, Y. H. Lai, W. Huang, *Chem. Mater*. **2001**, *13*, 1984. i) S. Beaupré, M. Leclerc, *Adv. Funct. Mater*. **2002**, *12*, 192. j) P. Herguth, X. Jiang, M. S. Liu, A. K.-Y. Jen, *Macromolecules* **2002**, *35*, 6094. k) M. S. Liu, J. Luo, A. K.-J. Jen, *Chem. Mater*. **2003**, *15*, 3496.

[11] a) R. Yang, R. Tian, Y. Yang, Q. Hou, Y. Cao, *Macromolecules* **2003**, *36*, 7453. b) Y.-H. Niu, Q. Hou, Y. Cao, *Appl. Phys. Lett*. **2003**, *82*, 2163. c) Y.-H. Niu, J. Huang, Y. Cao, *Adv. Mater*. **2003**, *15*, 807. d) J. Yang, C. Jiang, Y. Zhang, R. Yang, W. Yang, Q. Hou, Y. Cao, *Macromolecules* **2004**, *37*, 1211.

[12] C. Ego, D. Marsitzky, S. Becker, J. Zhang, A. C. Grimsdale, K. Müllen, J. D. MacKenzie, C. Silva, R. H. Friend, *J. Am. Chem. Soc*. **2003**, *125*, 437.

[13] X. Chen, J.-L. Liao, Y. Liang, M. O. Ahmed, H.-E. Tseng, S.-A. Chen, *J. Am. Chem. Soc*. **2003**, *125*, 636.

[14] a) C. Hosokawa, H. Higashi, H. Nakamura, T. Kusumoto, *Appl. Phys. Lett*. **1995**, *67*, 3853. b) J. M. Kauffman, G. Moyna, *J. Org. Chem*. **2003**, *68*, 839. c) J.-W. Park, S.-E. Lee, H.-C. Park, T.-G. Chung, H.-J. Seo, *Mater. Sci. Eng. C* **2004**, *24*, 103.

[15] S. Setayesh, D. Marsitzky, K. Müllen, *Macromolecules* **2000**, *33*, 2016.

[16] G. Wyszecki, W. S. Stiles, *Color Science*: *Concepts and Methods*, *Quantitative Data and Formulae*, John Wiley & Sons, New York **1982**, p. 259.

[17] J. Pei, J. Ni, X. H. Zhou, X. Y. Cao, Y. H. Lai, *J. Org. Chem*. **2002**, *67*, 4924.

[18] H.-J. Su, F.-I. Wu, C.-F. Shu, *Macromolecules* **2004**, *37*, 7197.

[19] N. Miyaura, A. Suzuki, *Chem. Rev*. **1995**, *95*, 2457.

[20] M. Ranger, D. Rondeau, M. Leclerc, *Macromolecules* **1997**, *30*, 7686.

[21] M. Grell, D. D. C. Bradley, M. Inbasekaran, E. P. Woo, *Adv. Mater*. **1997**, *9*, 798.

[22] S. Tokito, H. Tanaka, K. Noda, A. Okada, Y. Taga, *Appl. Phys. Lett*. **1997**, *70*, 1929.

[23] D. Eaton, *Pure Appl. Chem*. **1998**, *60*, 1107.

[24] A. W. Grice, D. D. C. Bradley, M. T. Bernius, M. Inbasekaran, W. W. Wu, E. P. Woo, *Appl. Phys. Lett*. **1998**, *73*, 629.

[25] J.-H. Kim, M. S. Liu, A. K.-J. Jen, B. Carlson, L. R. Dalton, C.-F. Shu, R. Dodda, *Appl. Phys. Lett*. **2003**, *83*, 776.

[26] S. W. Culligan, Y. Geng, S. H. Chen, K. Klubek, K. M. Vaeth, C. W. Tang, *Adv. Mater*. **2003**, *15*, 1176.

[27] Y.-Z. Lee, X. Chen, S.-A. Chen, P.-K. Wei, W.-S. Fann, *J. Am. Chem. Soc*. **2001**, *123*, 2296.

[28] a) D. Sainova, T. Miteva, H. G. Nothofer, U. Scherf, I. Glowacki, J. Ulanski, H. Fujikawa, D. Neher, *Appl. Phys. Lett*. **2000**, *76*, 1810. b) K.-H. Weinfurtner, H. Fujikawa, S. Tokito, Y. Taga, *Appl. Phys. Lett*. **2000**, *76*, 2502. c) E. J. W. List, R. Gunter, P. Scandiucci de Freitas, U. Scherf, *Adv. Mater*. **2002**, *14*, 374.

[29] J. Shi, C. W. Tang, C. H. Chen, *US Patent 5 645 948*, **1997**.

